

Daniel Korenciak - Miroslav Gutten - Juraj Adamec - Adam Glowacz - Adam Cichy*

ANALYSIS OF ENGINE KNOCK SENSOR

The paper deals with design of a simple device for the detection of this disorder. In the beginning of the paper the effect of the undesirable detonation combustion in internal combustion engines is described. An engine control unit monitors these detonations using piezoelectric knock sensors. With the control of these sensors the detonations can be objectively measured just outside the car on the test panels. If this component provides small amplitude of the output voltage it could happen that it would have been in the areas of the engine ignition combustion.

Keywords: knock sensor, diagnostic, testing device

1. Introduction

A knock sensor allows the engine to run with the ignition timing as far advanced as possible. The computer will continue to advance the timing until the knock sensor detects pinging. At that point the computer retards the ignition timing just enough for stopping the pinging.

The knock sensor responds to the spark knock caused by pre-detonation of the air/fuel mixture. As the flame moves to the front out of the spark plug ignition point, pressure waves in the chamber crash into the piston or cylinder walls resulting in a sound known as a knock or ping. This is caused by using a fuel with a low octane rating, overheating, or over advanced timing. It can sometimes be caused by hot carbon deposits on the piston or cylinder head that raise compression. A knock sensor is comprised of piezoelectric materials; crystals that when impacted, generate a voltage (same idea as a BBQ ignitor). This voltage is monitored by the computer, and when an irregularity is detected, the computer corrects timing in variable valve timing engines, or triggers Diagnostic Trouble Code in older vehicles [1-3].

2. Engine knocking

Detonation can be prevented by any or all of the following techniques:

- The use of a fuel with high octane rating, which increases the combustion temperature of the fuel and reduces the proclivity to detonate;
- enriching the air-fuel ratio which alters the chemical reactions during combustion, reduces the combustion temperature and increases the margin above detonation;
- reducing peak cylinder pressure by decreasing the engine revolutions (e.g., shifting to a higher gear, there is also evidence that knock occurs more easily at high rpm than low regardless of other factors);
- decreasing the manifold pressure by reducing the throttle opening, boost pressure or
- reducing the load on the engine.

At detonation combustion occurs to rapid changes in pressure (Figure 1). These fast pressure changes; generated by sound waves, which are in modern automobiles captured by the knock sensor [4].

3. Adaptive knock control

At dynamic engine transients, mismatches of the ignition angle occur resulting in increased knock occurrence rates. The response time of knock control can be reduced by a feed-forward control angle $\alpha_i(n)$ stored in an adaptive ignition angle map. Contrary to lambda control, a successful global error model has not yet been found. The values of the ignition angle map must

* ¹Daniel Korenciak, ¹Miroslav Gutten, ²Juraj Adamec, ³Adam Glowacz, ⁴Adam Cichy

¹Department of Measurements and Applied Electrical Engineering, Faculty of Electrical Engineering, University of Zilina, Slovakia

²Department of Mechatronics and Electronics, Faculty of Electrical Engineering, University of Zilina, Slovakia

³Automatics, Computer Science and Biomedical Engineering, Faculty of Electrical Engineering, AGH University of Science and Technology, Krakow, Poland

⁴Faculty of Electrical Engineering, Silesian University of Technology, Gliwice, Poland

E-mail: gutten@fel.uniza.sk

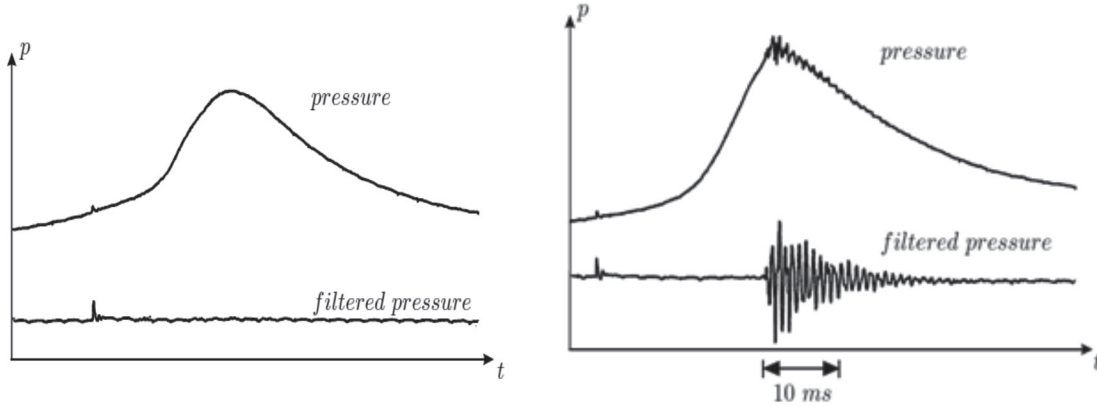


Figure 1 Bandpass output signal: a) non-knocking combustion, b) knocking combustion [1]

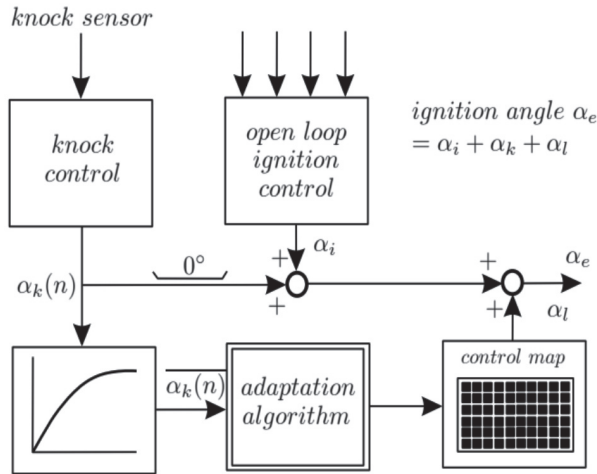


Figure 2 Knock control with feed-forward adaptive ignition angle map [5]

therefore be adapted in every individual engine operating point for all cylinders.

The ignition angle at one cylinder is the sum:

$$\alpha_e(n) = \alpha_i(n) + \alpha_k(n) + \alpha_l(n) \quad (1)$$

where α_e is the effective ignition angle, α_i is the open loop ignition angle from fixed map, α_k is the knock control ignition angle, and α_l is the learned ignition angle from adaptive map.

The average knock control ignition angle $\alpha_k(n)$ is the basis to teach the adaptive ignition angle map $\alpha_l(n)$ into the direction of retarding. A fixed advance angle α_a is superimposed to the teaching process providing a forgetting function of the taught angles. The learned ignition angle is

$$\alpha_l(n) = (1 - k_l)\alpha_l(n-1) + k_l(\bar{\alpha}_k(n-1) + \alpha_a(n-1)) \quad (2)$$

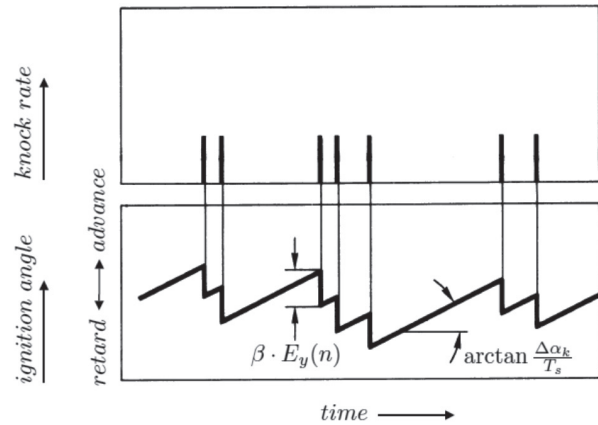


Figure 3 Control of knock occurrence rate by ignition angle shifting [5]

The factor k_l determines how fast the learning process is [5]. The illustration of knock control with feed-forward adaptive ignition angle map is shown in Figure 2.

The usual actuation is a retardation of the ignition angle, shifting the energy conversion process backwards and thus reducing peak pressures and temperatures. An alternative input may be to lower the boost pressure of a turbo charger. The knock control ignition angle is calculated at discrete combustion cycles n as

$$\alpha_k(n) = \alpha_k(n-1) + \Delta \alpha_k - \beta \cdot \Delta E_y(n) \quad (3)$$

where $\Delta \alpha_k$ is a permanent ignition angle advance, and $\beta \Delta E_y(n)$ the ignition angle retard at knocking. A typical control cycle is shown in Figure 3. The knock control ignition angle $\alpha_k(n)$ is added to the ignition angle obtained from the ignition map.

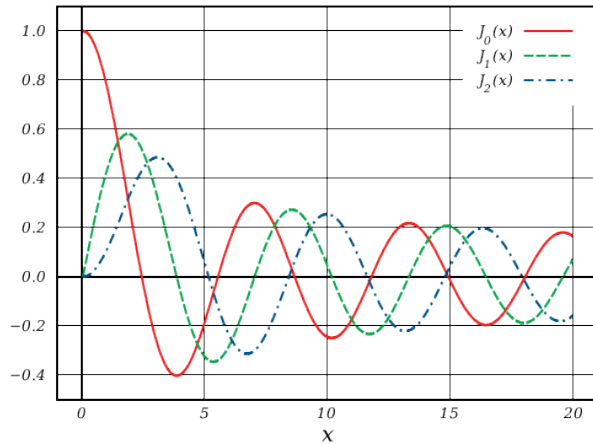


Figure 4 Plot of Bessel function of the first kind, $J_\alpha(x)$ [6]

4. Knock sensor output signal

Sound waves generated by detonation during combustion have a frequency of between 6 to 20 kHz. Their frequency can be approximated by:

$$f_{mn} = c_0 \sqrt{\frac{v}{273}} \cdot \frac{\beta_{mn}}{d} \quad (4)$$

where c_0 is the sound propagation velocity at 273 K, v is the temperature within combustion chamber, d is the cylinder diameter, β_{mn} is the Bessel function (e.g. $\beta_{10}=0.5861$, $\beta_{20}=0.9722$, $\beta_{30}=1.2197$).

From the parameters $c_0 = 330$ m/s, $v = 2500$ K, $d = 0.089$ m we can calculate the knock resonance frequencies $f_{10} = 6.6$ kHz, $f_{20} = 10.9$ kHz, $f_{30} = 13.7$ kHz.

Bessel functions are defined as the solutions $y(x)$ of Bessel's differential equation:

$$x^2 \frac{d^2 y}{dx^2} + x \frac{dy}{dx} + (x^2 - a^2)y = 0 \quad (5)$$

It is possible to define the function by its Taylor series expansion around $x = 0$:

$$J_\alpha(x) = \sum_{n=0}^{\infty} \frac{(-1)^n}{n! \Gamma(m + \alpha + 1)} \left(\frac{x}{2}\right)^{2n + \alpha} \quad (6)$$

where Γ is the gamma function, a shifted generalization of the factorial function to non-integer values.

The Bessel function of the first kind is an entire function if α is an integer (Figure 4). The graphs of Bessel functions look roughly like oscillating sine or cosine functions that decay proportionally to $1/\sqrt{x}$ (see also their asymptotic forms below), although their roots are not generally periodic, except asymptotically for large x .

The Taylor series indicates that $-J_1(x)$ is the derivative of $J_0(x)$, much like $-\sin(x)$ is the derivative of $\cos(x)$; more generally, the derivative of $J_n(x)$ can be expressed in terms of $J_{n\pm 1}(x)$ by the identities below [7].

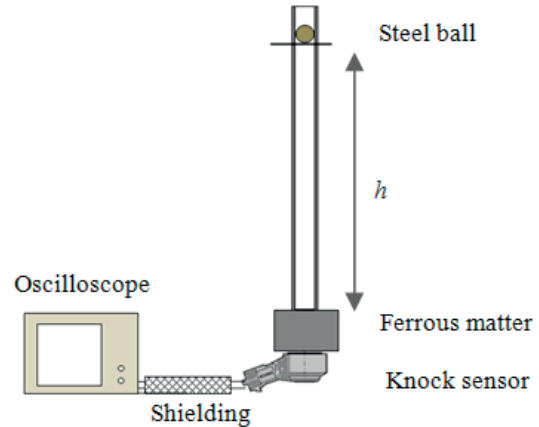


Figure 5 Testing device

A simple but effective test knock sensor is shown in Figure 5. The sensor is attached to a metal cylindrical body. The plastic tube is adjusted so as to allow for the impact of the metal balls of different heights h .

Impact of ball on a metallic material with a height of 1.8 cm and a diameter of 3.4 cm generates sound waves. These waves are captured by a knock sensor. The output voltage signal, which is shown in Figure 6, corresponds with Bessel function.

Using a measuring apparatus consisting of an oscilloscope, metal impact surface, plastic tube with adjustable height and metal ball, we tested the response the knock sensor from Bosch which was used in VW Golf. The response was stored in oscilloscope and then the values of voltage were shown in Figure 6.

The principally schematic of sound waves spreading in metal environment created by ball impact on surface of metal material is shown in Figure 7. The knock sensor is placed on the bottom of the metal plate. In the middle of the plate is screw which is tighten to rated torque. This arrangement provides the best possible transfer of mechanical waves on the surface of the sensor [8].

The diagnostic of knock sensor is based on the response of knock sensor on the first two extremes of the measured signal. The amplitude of the signal shows level of sensor sensitive and what is the shape of the sensor response. From the measured values we could specify a "normal curve" which shows how big the voltage response should be from this kind of sensor. It replaces the mounting used by the manufacturer for this sensor [9].

The value of the generated voltage depends on the gravitational potential energy of the falling bullet [10]:

$$E_p = m \cdot g \cdot h \quad (7)$$

where m is the mass of the body (2050mg), g is the acceleration due to gravity (9.81 m/s^2), h is the height of the body above the surface (5 cm, 10 cm, 15 cm, 20 cm, 25 cm, 30 cm, 40 cm, 50 cm).

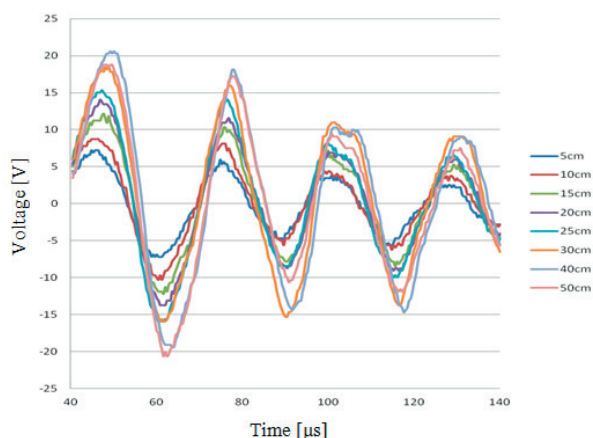


Figure 6 Output voltage of the sensor

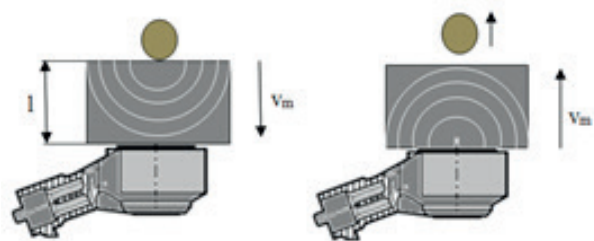


Figure 7 Sound reflection after the bullets' impact

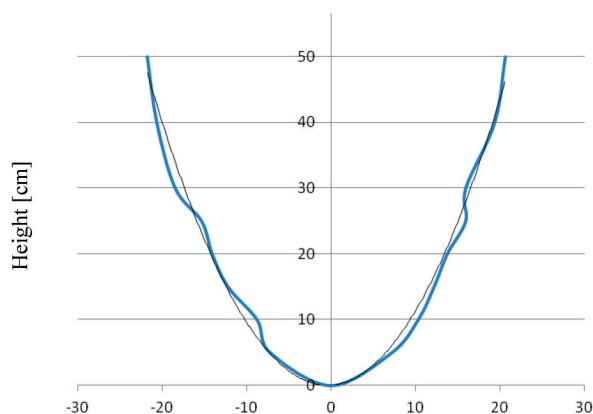


Figure 8 Output voltage depending on the amount of the impact

Calculation of the output voltage can be realized by means of the formula:

$$U = 20 \cdot \log(E_p + 1) \quad (8)$$

Restriction reflecting the sound waves can be accomplished by changing the shape of a metallic material. An experiment was conducted where a steel ball was thrown directly at the sensor. In this impact we can already consider the Bessel function [11].

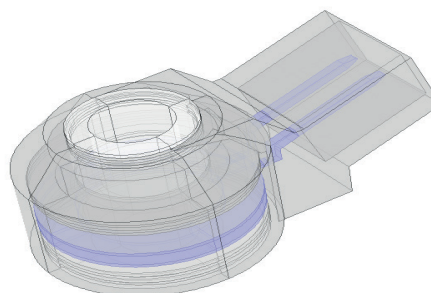


Figure 9 3D model of knock sensor

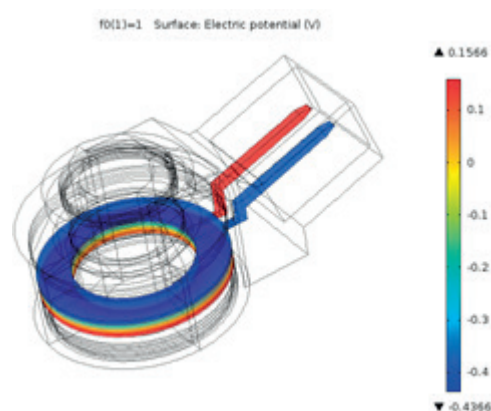


Figure 10 Output potentials of sensor with 1N of force affecting on piezoelectric element

Figure 9 shows the 3D model of the knock sensor. It is modelled on materials composition and functions like in real use. The cover of the sensor is made from plastic and electrodes are made from metal. Inner pressure sensitive layer is simulated by a crystal. On this model it is affecting outer force. The model is detailed because the response of the crystal is influenced by the sensor cover and the body of the sensor too. Figure 10 shows the knock sensor simulation in the COMSOL [12] at pressure of 1N. In Figure 10 we can see an electric potential of the sensor.

5. Conclusion

A construction of the testing device for the knock sensor suitable for diagnostics of the knock combustion in internal combustion engines has been presented.

The output signal of the presented sensor has been described by Bessel functions. Using the first voltage extremes on the characteristics from Figure 6 it is possible to create a reference for the evaluation of the polynomial residue. It should be taken into account that the velocity of sound in the air is 330 m/s. This sound impinges on the walls of the combustion chamber and is detected by the sensor. The resonant frequency of the clicking of the motor is usually in the range from 5 kHz to 15 kHz. The

sensor worked in the field to 37 kHz, which shall be taken into account on an own sensor resonance.

Acknowledgment

This work was supported by the Grant Agency VEGA from the Ministry of Education of Slovak Republic under contract 1/0602/17.

References

1. GUPTA, H. N.: Fundamentals of Internal Combustion Engines. PHI Learning, 169–173, 2006.
2. CLINE, A. W.: Engine Basics: Detonation and Pre-Ignition. Accessed June 2007.
3. FAYETTE TAYLOR, Ch.: Internal Combustion Engine in Theory and Practice, Second Edition, Revised, Volume 2, Chapter 2 “Detonation and Preignition”. MIT Press, pp. 34–85, 1985.
4. Modeling Pressure Oscillations under Knocking Conditions: A Partial Differential Wave Equation Approach. SAE Technical Paper n. 2010-01-2185, 2010.
5. KIENCKE, U., NIELSEN, L.: Automotive Control Systems for Engine, Driveline, and Vehicle. Springer Berlin, Heidelberg, 2005.
6. GRANDSHTEYN, I. S., RYZHIK, I. M., JEFFREY, A., ZWILLINGER, D. (Eds): Table of Integrals, Series, and Products, Seventh edition. Academic Press, 2007.
7. TEMME, N. M.: Special Functions: An Introduction to the Classical Functions of Mathematical Physics, Second Edition. Wiley, New York, pp. 228–231.
8. SIMKO, M., CHUPAC, M.: Non-Destructive Method of Measurement of Radio Transmitters Antenna Systems. Elektronika ir Elektrotechnika/Electronics and Electrical Engineering, 107(1), 33-36, 2011.
9. CONGBO, Y., ZHENDONG, Z., ZHIYUAN, L.: Experimental Research and Design for Electronic Control Injector Test about Flow Characteristic. Journal of Agricultural Mechanization Research, 12, 194-196, 2007.
10. LONGFA, X., ZHENDONG, Z., HUI, G., etc: Research on the Opening and Closing Times of an Electromagnetic Injector. Journal of University of Shanghai for Science and Technology, 32, 297-301, 2010.
11. CHEN L., ZHANG, Z.: Study on the Measurement of Dynamic Characteristics for Automotive Electronic Fuel Injector. Proceeding of International Conference on Transportation, Mechanical, and Electrical Engineering (TMEE), China, 2011.
12. CONSOL [online]. Available: <http://www.comsol.com>.